Scattering sound field prediction over periodic facing walls containing rectangular cavities

Adel Khanfir, Adil Faiz, Joël Ducourneau, Jacques Chatillon

ACOUSTICS 2012

Scattering sound field prediction over periodic facing walls containing rectangular cavities

A. Khanfir[a], A. Faiz[b], J. Ducourneau[b] and J. Chatillon[a]

[a]INRS, 1, Rue Morvan, 54519 Vandoeuvre-Lès-Nancy, France
[b]Faculté de Pharmacie de Nancy, 5, rue Albert Lebrun, 54001 Nancy, France
adel.khanfir@inrs.fr

The "Institut national de recherche et de sécurité" (INRS) is interested in reducing hearing risks in industrial workplaces by improving in situ noise conditions. INRS proposes appropriate solutions for improving the acoustic treatment of facings for workplace noise control. This requires development of theoretical and experimental methods of acoustically characterizing wall facings present in industrial rooms. Such walls, which possess periodic or aperiodic relief, scatter sound waves. This work consists in developing a theoretical model to predict the acoustic pressure field reflected and scattered over a periodic facing containing parallel rectangular cavities. Originally, the model was based on a study of thick slits in electromagnetism. It was adapted to study the acoustic behavior of a rectangular cavity by blocking off the bottom of the slit. Then, the model was generalized for several joint cavities by taking into account effects of coupling. It was compared with experimental results obtained in a semi-anechoic room for a periodic facing containing three parallel rectangular cavities insonified by an incident spherical acoustic field. The observed concordance between the numerical and experimental results supports the validity of our model over a wide spectral range.

1 Introduction

Acoustic characterization of surfaces in industrial workplaces is necessary for predicting the sound pressure level at specific locations, for improving acoustic treatment and providing suitable noise control solutions. Workshop wall facings mostly feature geometric and/or acoustic irregularities, usually comprising rectangular cavities created by windows, doors and congesting furniture, which induce a scattered acoustic field.

The purpose of this work is to predict this scattered field over a wide frequency range, for a rectangular cavity. K. Hongo et al [1] and H. Serizawa et al [2] use the Kobayashi Potential (KP) method for determining the acoustic field diffracted by a rectangular aperture in an infinitely large screen. K. Hongo et al. [5, 6] used the KP method to investigate the electromagnetic field diffracted by an array of N slits and by N parallel plate wave-guides respectively. In this study, the KP method was adapted to predict the scattered acoustic field generated by several parallel rectangular cavities in an infinitely large rigid screen.

2 Statement of the problem

2.1 Study of a single cavity

Consider a rectangular cavity in an infinitely large, rigid, thick screen. The cavity size is $2a \times 2b \times d$. Let η_{ad} be the characteristic admittance of the bottom of the cavity, Φ_{inc}^{pl} be the incident acoustic field and Φ_r be the specular reflected wave generated by the flange given by $D^c = \{(x,y)/|x| > a, |y| > b\} \subset \mathbb{R}^2$ and $z = 0$. D is the complement of the section of space D^c. Φ_d is the diffracted acoustic wave generated by the cavity. Φ_w is the acoustic modal field propagating in the cavity. These features are shown in figure 1.

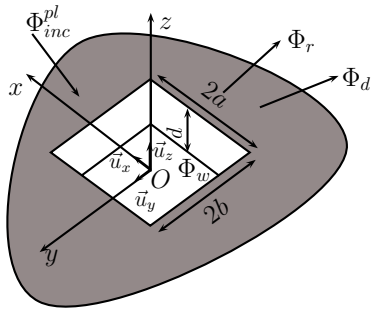

Figure 1: Geometry of the studied cavity and different acoustic fields

The expressions of the incident, the specular reflected plane waves, and the modal field, are known to be (1)-(3) respectively in the frame of reference (O, x, y, z). According to the KP method the diffracted acoustic field is given by the equation (4) [1, 2].

$$\Phi_{inc}^{pl} = Ae^{jk_x x}e^{jk_y y}e^{jk_z z} \tag{1}$$

$$\Phi_r = Ae^{jk_x x}e^{jk_y y}e^{-jk_z z} \tag{2}$$

$$\Phi_w = \sum_{p\geq 0}\sum_{q\geq 0}\cos\left(\frac{p\pi}{2}(\xi+1)\right)\cos\left(\frac{q\pi}{2}(\eta+1)\right) \times \left(E_{pq}e^{-\gamma_{pq}z} + F_{pq}e^{\gamma_{pq}z}\right) \tag{3}$$

$$\Phi_d = \sum_{m,n\geq 0}\iint_{\mathbb{R}_+^2}\left(A_{mn}\Phi_{cc}^{(m,n)} + B_{mn}\Phi_{cs}^{(m,n)} + C_{mn}\Phi_{sc}^{(m,n)} + D_{mn}\Phi_{ss}^{(m,n)}\right)e^{-\sqrt{\frac{\alpha^2}{a^2}+\frac{\beta^2}{b^2}-k^2}z}\,d\alpha\,d\beta \tag{4}$$

where $\vec{k} = k_x\vec{u_x} + k_y\vec{u_y} + k_z\vec{u_z}$ is the reflected wave vector, $\xi = \frac{x}{a}$, $\eta = \frac{y}{b}$ and $\gamma_{p,q} = \sqrt{(\frac{p\pi}{2a})^2 + (\frac{q\pi}{2b})^2 - k^2}$. A_{mn}, B_{mn}, C_{mn}, D_{mn}, E_{pq} and F_{pq} are unknown modal amplitudes. With:

$$\Phi_{cc}^{(m,n)} = \frac{J_{2m}(\alpha)J_{2n}(\beta)cos(\alpha\xi)cos(\beta\eta)}{\sqrt{\frac{\alpha^2}{a^2}+\frac{\beta^2}{b^2}-k^2}} \tag{5}$$

$$\Phi_{cs}^{(m,n)} = \frac{J_{2m}(\alpha)J_{2n+1}(\beta)cos(\alpha\xi)sin(\beta\eta)}{\sqrt{\frac{\alpha^2}{a^2}+\frac{\beta^2}{b^2}-k^2}} \tag{6}$$

$$\Phi_{sc}^{(m,n)} = \frac{J_{2m+1}(\alpha)J_{2n}(\beta)sin(\alpha\xi)cos(\beta\eta)}{\sqrt{\frac{\alpha^2}{a^2}+\frac{\beta^2}{b^2}-k^2}} \tag{7}$$

$$\Phi_{ss}^{(m,n)} = \frac{J_{2m+1}(\alpha)J_{2n+1}(\beta)sin(\alpha\xi)sin(\beta\eta)}{\sqrt{\frac{\alpha^2}{a^2}+\frac{\beta^2}{b^2}-k^2}} \tag{8}$$

The various unknown amplitudes are determined by enforcing the boundary conditions (9)-(11).

$$\frac{\partial}{\partial z}\left(\Phi_{inc}^{pl} + \Phi_r + \Phi_d\right) = \frac{\partial}{\partial z}\Phi_w,\ (x,y) \in D,\ z = 0 \tag{9}$$

$$\Phi_{inc}^{pl} + \Phi_r + \Phi_d = \Phi_w,\ (x,y) \in D,\ z = 0 \tag{10}$$

$$\frac{\partial \Phi_w}{\partial z} - jk\eta_{ad}\Phi_w = 0,\ (x,y) \in D,\ z = -d \tag{11}$$

We expand the trigonometric functions in the equation (9) in terms of Jacobi's polynomials, $G^{(2,\frac{3}{2})}(x)$ for the sine function and $G^{(2,\frac{1}{2})}(x)$ for the cosine function, to project the resulting equations into the functional space defined by the same polynomials. The equation (10) is projected into the functional space defined by trigonometrical functions. The

equation (11) allows us to eliminate one of the unknown amplitudes: F_{pq} or E_{pq}. The resulting equations build up a system of linear equations enabling us to determine the unknown amplitudes: A_{mn}, B_{mn}, C_{mn}, and D_{mn}. This system is given by equations (12)-(15).

$$[A_{mn}][G(2m, 2n, 2s+1, 2t+1)] = [\Lambda(2s+1, 2t+1)] \quad (12)$$

$$[B_{mn}][G(2m, 2n+1, 2s+1, 2t+2)] = [\Lambda(2s+1, 2t+2)] \quad (13)$$

$$[C_{mn}][G(2m+1, 2n, 2s+2, 2t+1)] = [\Lambda(2s+2, 2t+1)] \quad (14)$$

$$[D_{mn}][G(2m+1, 2n+1, 2s+2, 2t+2)] = [\Lambda(2s+2, 2t+2)] \quad (15)$$

$$s, t = 0, 1, 2, \cdots$$

Where:

$$\begin{aligned} &G(2m+\mu, 2n+\nu, 2s+1+\mu, 2t+1+\nu) \\ &= \iint_{\mathbb{R}_+^2} \frac{J_{2m+\mu}(\alpha) J_{2s+1+\mu}(\alpha) J_{2n+\nu}(\beta) J_{2t+1+\nu}(\beta)}{\alpha\beta \sqrt{\frac{\alpha^2}{a^2} + \frac{\beta^2}{b^2} - k^2}} \, d\alpha \, d\beta \\ &- \sum_{p,q\geq 0} \left(\frac{1}{\epsilon_{2p+\mu}\epsilon_{2q+\nu}\gamma_{2p+\mu,2q+\nu}} \frac{\Gamma^+_{2p+\mu,2q+\nu}}{\Gamma^-_{2p+\mu,2q+\nu}} \right. \\ &\times \frac{J_{2m}(\frac{2p+\mu}{2}\pi) J_{2s+1+\mu}(\frac{2p+\mu}{2}\pi)}{\frac{2p+\mu}{2}} \\ &\left. \times \frac{J_{2n}(\frac{2q+\nu}{2}\pi) J_{2t+1+\nu}(\frac{2q+\nu}{2}\pi)}{\frac{2q+\nu}{2}} \right) \end{aligned} \quad (16)$$

$$\begin{aligned} &\Lambda(2s+1+\mu, 2t+1+\nu) \\ &= -2j^{\mu+\nu} A \frac{J_{2s+1+\mu}(k_x a)}{k_x a} \frac{J_{2t+1+\nu}(k_y b)}{k_y b} \end{aligned} \quad (17)$$

With:

$$\Gamma^{\pm}_{p,q} = 1 \pm \frac{\gamma_{pq} + jk\eta_{ad}}{\gamma_{pq} - jk\eta_{ad}} e^{2\gamma_{pq} d} \quad (18)$$

$$\epsilon_p = \begin{cases} 2 & \text{if } p = 0 \\ 1 & \text{else} \end{cases} \quad (19)$$

The double integrals in equation (4) are transformed into polar coordinates and then divided into two regions: real and imaginary parts. The integral in each region is evaluated using the Cubature method [3].

2.2 Study of several cavities

Consider now that we have a array of N rectangular cavities. We then have N diffracted fields, generated by respective ones of the cavities, and N modal acoustic fields propagating inside the N cavities. Thus, we have $6N$ unkown amplitudes. In order to determine them, we apply the following boundary conditions for the i^{th} cavity:

$$\frac{\partial}{\partial z}\left(\Phi^{pl}_{inc} + \Phi_r + \Phi^i_d + \sum_{j\neq i} \Phi^j_d \right) = \frac{\partial}{\partial z} \Phi^i_w, (x_i, y_i) \in D, z = 0 \quad (20)$$

$$\Phi^{pl}_{inc} + \Phi_r + \Phi^i_d + \sum_{j\neq i} \Phi^j_d = \Phi^i_w, \ (x_i, y_i) \in D, \ z = 0 \quad (21)$$

$$\frac{\partial \Phi^i_w}{\partial z} - jk\eta^i_{ad} \Phi^i_w = 0, \ (x_i, y_i) \in D, \ z = -d_i \quad (22)$$

Where $D = \{(x, y) / |x_i| < a_i, \ |y_i| < b_i\} \subset \mathbb{R}^2$ represent the domain of the cavities. D^c is the complement of D.

The total field above the i^{th} cavity contains the incident field Φ^{pl}_{inc}, the specular reflected field Φ_r, the diffracted field Φ^i_d generated by i^{th} element itself and the other diffracted fields $\sum_{j\neq i} \Phi^j_d$ generated by its neighboring cavities: all the j^{th} cavities excluding the i^{th} one. This term illustrates the contribution from other cavities in the generation of the field diffracted by the i^{th} cavity. It corresponds to the coupling between the different cavities contained in the wall facing.

To apply the conditions (20)-(21) we use the relationships (23) and (26) between the various local coordinates.

$$x = x_i + \delta_{x_i} \quad (23)$$

$$y = y_i + \delta_{y_i} \quad (24)$$

$$x_j = x_i + \delta_{x_{ij}} \quad (25)$$

$$y_j = y_i + \delta_{y_{ij}} \quad (26)$$

Where $(\delta_{x_i}, \delta_{y_i})$ are the coordinates of the i^{th} local frame (O_i, x_i, y_i, z) centre in the reference frame (O, x, y). $\delta_{x_{ij}}$ (respectively $\delta_{y_{ij}}$) represents the distance between the centres of the i^{th} and the j^{th} local frames along the x axis (respectively y axis), given by:

$$\delta_{x_{ij}} = \delta_{x_i} - \delta_{x_j} \quad (27)$$

$$\delta_{y_{ij}} = \delta_{y_i} - \delta_{y_j} \quad (28)$$

We apply the same procedure as a simple cavity and we obtain the system of matrix equations to calculate the amplitudes A^i_{mn}, B^i_{mn}, C^i_{mn} and D^i_{mn} of the i^{th} cavity:

$$\begin{aligned} &[A^i_{mn}][G^{0_i,0_i}] + \sum_{j\neq i} \left([A^j_{mn}][G^{0_i,0_i}_{0_j,0_j}] + [B^j_{mn}][G^{0_i,0_i}_{0_j,1_j}] \right. \\ &\left. + [C^j_{mn}][G^{0_i,0_i}_{1_j,0_j}] + [D^j_{mn}][G^{0_i,0_i}_{1_j,1_j}] \right) = [\Lambda^{0_i,0_i}] \end{aligned} \quad (29)$$

$$\begin{aligned} &[B^i_{mn}][G^{0_i,1_i}] + \sum_{j\neq i} \left([A^j_{mn}][G^{0_i,1_i}_{0_j,0_j}] + [B^j_{mn}][G^{0_i,1_i}_{0_j,1_j}] \right. \\ &\left. + [C^j_{mn}][G^{0_i,1_i}_{1_j,0_j}] + [D^j_{mn}][G^{0_i,1_i}_{1_j,1_j}] \right) = [\Lambda^{0_i,1_i}] \end{aligned} \quad (30)$$

$$\begin{aligned} &[C^i_{mn}][G^{1_i,0_i}] + \sum_{j\neq i} \left([A^j_{mn}][G^{1_i,0_i}_{0_j,0_j}] + [B^j_{mn}][G^{1_i,0_i}_{0_j,1_j}] \right. \\ &\left. + [C^j_{mn}][G^{1_i,0_i}_{1_j,0_j}] + [D^j_{mn}][G^{1_i,0_i}_{1_j,1_j}] \right) = [\Lambda^{1_i,0_i}] \end{aligned} \quad (31)$$

$$\begin{aligned} &[D^i_{mn}][G^{1_i,1_i}] + \sum_{j\neq i} \left([A^j_{mn}][G^{1_i,1_i}_{0_j,0_j}] + [B^j_{mn}][G^{1_i,1_i}_{0_j,1_j}] \right. \\ &\left. + [C^j_{mn}][G^{1_i,1_i}_{1_j,0_j}] + [D^j_{mn}][G^{1_i,1_i}_{1_j,1_j}] \right) = [\Lambda^{1_i,1_i}] \end{aligned} \quad (32)$$

Where:

$$\begin{aligned} G^{\mu_i,\nu_i} &= \iint_{\mathbb{R}_+^2} \frac{J_{2m+\mu_i}(\alpha) J_{2s+1+\mu_i}(\alpha) J_{2n+\nu_i}(\beta) J_{2t+1+\nu_i}(\beta)}{\alpha\beta \sqrt{\alpha^2 + (\frac{a_i}{b_i}\beta)^2 - (ka_i)^2}} \, d\alpha \, d\beta \\ &- \sum_{p,q\geq 0} \left(\frac{\pi^2}{\epsilon_{2p+\mu_i}\epsilon_{2q+\nu_i}\gamma_{2p+\mu_i,2q+\nu_i}} \frac{\Gamma^{+i}_{2p+\mu_i,2q+\nu_i}}{\Gamma^{-i}_{2p+\mu_i,2q+\nu_i}} \right. \\ &\left. \times \frac{J_{2m}(\frac{2p+\mu_i}{2}\pi) J_{2s+1+\mu_i}(\frac{2p+\mu_i}{2}\pi)}{\frac{2p+\mu_i}{2}\pi} \right. \end{aligned}$$

$$\times \frac{J_{2n}(\frac{2q+\nu_i}{2}\pi)J_{2t+1+\nu_i}(\frac{2q+\nu_i}{2}\pi)}{\frac{2q+\nu_i}{2}\pi}\Bigg) \quad (33)$$

$$s,t = 0,1,2,\cdots$$

$$G^{\mu_i,\nu_i}_{\mu_j,\nu_j} = (-1)^{\mu_j+\nu_j}$$

$$\times \iint_{\mathbb{R}^2_+} \frac{J_{2m+\mu_j}(\alpha)J_{2s+1+\mu_i}(\frac{a_i}{a_j}\alpha)J_{2n+\nu_j}(\beta)J_{2t+1+\nu_i}(\frac{b_i}{b_j}\beta)}{\frac{a_i}{a_j}\alpha\frac{b_i}{b_j}\beta\sqrt{\alpha^2+(\frac{a_j}{b_j}\beta)^2-(ka_j)^2}}$$

$$\times \cos\left(\frac{\delta_{x_{ij}}}{a_j}\alpha+(\mu_i+\mu_j)\frac{\pi}{2}\right)\cos\left(\frac{\delta_{y_{ij}}}{b_j}\beta+(\nu_i+\nu_j)\frac{\pi}{2}\right)d\alpha d\beta \quad (34)$$

$$\Lambda^{\mu_i,\nu_i} = -2j^{\mu_i+\nu_i}A\frac{J_{2s+1+\mu_i}(k_xa_i)}{k_xa_i}\frac{J_{2t+1+\nu_i}(k_yb_i)}{k_yb_i} \quad (35)$$

With:

$$\Gamma^{\pm i}_{pq} = 1 \pm \frac{\gamma^i_{pq}+jka_i\eta^i_{ad}}{\gamma^i_{pq}-jka_i\eta^i_{ad}}e^{2\gamma^i_{pq}d_i} \quad (36)$$

$$\gamma^i_{pq} = \sqrt{(\frac{p\pi}{2})^2+(\frac{a_i}{b_i}\frac{q\pi}{2})^2-(ka_i)^2} \quad (37)$$

3 Results and discussion

To validate the model, sound pressure profiles above two wall facings were measured.

- The first was formed by a $(46.0\times48.2\times21.1)\,cm^3$ rigid cavity.
- The second was a periodic array of $(50.3\times48.4\times21.1)\,cm^3$ rigid cavities. The periodicity was $34.4\,cm$ along the x axis. The reference frame is centered on the central cavity.

3.1 Experimental procedure

Measurements were taken under free-field conditions in the INRS semi-anechoic chamber. The cavities' bottoms were considered infinitely rigid (steel or tiles). Profiles were formed by tiled polystyrene blocks to ensure a high acoustic reflection coefficient.

The sound source used for the test was a horn with a $15\,mm$ outlet diameter. A $10\,cm$ diameter Pioneer TS $E1077$ loudspeaker was fixed between the horn and the cylindrical body. The source emitted spherical waves [4].

The acoustic source was connected to a B&K 1405 noise generator through a Power APK 2000 amplifier and a Yamaha GQ 1031 Graphic Equalizer to generate white noise. B&K 4935 1/4" microphones were used for acquisition, connected to a B&K 2694 Deltatron conditioner. The acquisition system was a NetdB of the 01dB-Metravib company (Figure 2). Signal acquisition was performed at a $25,600\,Hz$ sampling frequency for $30\,s$.

The sound pressure profile was measured by 45 sensors along the x axis. Measurement was performed in three stages, for three juxtaposed positions of an antenna fitted with 15 small 1/4" microphones. These were spaced apart at $5.5\,cm$ intervals and their positions were chosen such that the central microphone of the 45-sensor virtual array was positioned directly below the loudspeaker at $0.2\,m$ above the studied wall facing (see figure 3).

For the experimental system, we opted for a spherical acoustic incident wave, which was decomposed into a plane wave spectrum. The total diffracted field was obtained by summing all fields generated by the respective plane waves (see section 3.2)

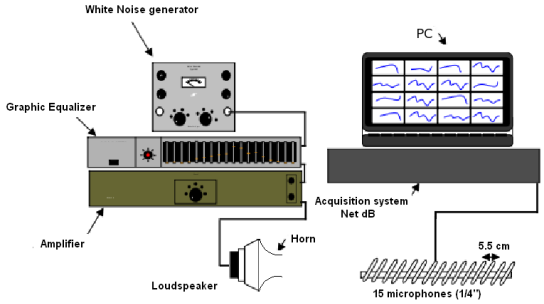

Figure 2: Experimental device

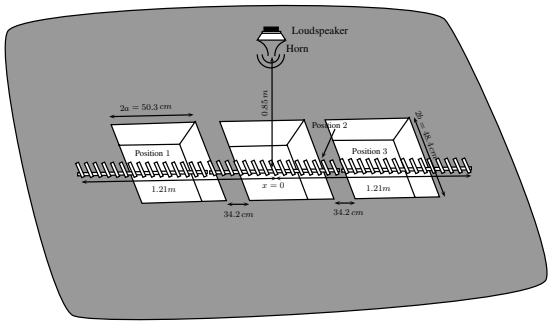

Figure 3: Experimental procedure for the array of three cavities

In simulation, the matrices $[G^{\mu_i,\nu_i}]$ and $[G^{\mu_i,\nu_i}_{\mu_j,\nu_j}]$ in equations (29)-(32) were truncated by $S^2\times S^2$. Where S is the maximum value of m, n, s, and t. The decomposition into plane wave spectrum were integrated into the systems of the matrix equations (29)-(32) The sizes of the matrices $[A_{mn}]$, $[B_{mn}]$, $[C_{mn}]$, $[D_{mn}]$ and $[\Lambda^{\mu_i,\nu_i}]$ are $n_xn_y\times S^2$. n_x and n_y are the numbers of FFT samples along the x and y axis respectively (see section 3.2).

3.2 Principle of incident acoustic field decomposition

This technique involves expanding a complex wave field into the sum of an infinite number of plane waves. The plane wave amplitudes $\tilde{A}$ are given by the following decomposition process at $z=0$:

$$\tilde{A}(k_x,k_y,0) = \iint_{\mathbb{R}^2}\Phi^{sph}_{inc}(x,y,z=0)e^{-j(k_xx+k_yy)}dxdy \quad (38)$$

Where Φ^{sph}_{inc} is the incident acoustic field to be decomposed.

The 2-dimensional Fourier transform was numerically determined using a Fast Fourier Transform (FFT) algorithm. Spatial sampling must satisfy Shannon's theorem:

$$\Delta x < \frac{c}{2f},\ \Delta y < \frac{c}{2f} \quad (39)$$

The number of FFT samples n_x and n_y must be squares for the FFT algorithm to give acceptable results. The dimensions L_x and L_y of the sampling grid must be large enough to consider the incident field negligible outside.

$$n_x = 2^{Int^+(log_2(\frac{L_x}{\Delta x}))} \quad (40)$$

$$n_y = 2^{Int^+(log_2(\frac{L_y}{\Delta y}))} \quad (41)$$

Where $Int^{+}(var) = Int(var) + 1$, and $Int(var)$ is the integer part of the decimal number var.

3.3 Results

Figure 4 shows the various acoustic pressure moduli obtained with the model and the experiment for frequencies of $500\,Hz$, $1100\,Hz$, $1600\,Hz$ and $3100\,Hz$ along the x axis for the single cavity. Figure 5 shows the various acoustic pressure moduli obtained with the model and the experiment for frequencies of $230\,Hz$, $500\,Hz$ $1100\,Hz$ and $1500\,Hz$ along the x axis for the periodic array. All these acoustic pressure profiles are normalized with respect to the central microphone measurement.

We observe that these acoustic pressure moduli are fairly symmetrical with respect to the center of the loudspeaker.

The acoustic pressure moduli become more irregular as the frequency increases. This phenomenon is justified by the more directive scattering at these frequencies. Another reason is that the size of the edges becomes large compared to the wavelength, increasing the scattering.

We note in the case of the periodic array that coupling is more important at the frequency $230\,Hz$. We suppose that the interactions of acoustic coupling between the cavities are larger in low frequencies because the acoustic radiation of a cavity can easily disrupt the acoustic field insonifying the neighboring cavities at these frequencies. At higher frequencies, the coupled and uncoupled fields become very close. This allows us to say that the coupling decreases at high frequencies. We suppose that at such frequencies, the acoustic radiation of a cavity becomes more directive. It has less ability to disrupt the acoustic field insonifying the neighboring cavities. These hypotheses will soon be verified by an experimental study.

Measurements at greater distances from the surface were not taken because the model was designed for infinite surfaces. We placed the spherical source close to the studied profile to prevent acoustic boundary phenomena associated with the finite dimensions of the studied profiles. It would have been difficult to position the microphone further from the surface under these conditions. Up to $3100\,Hz$, the curves show a good concordance between the numerical and experimental results. Processing was limited to the three highest frequencies because the computing load limit was reached for this frequency (or just above).

A root mean square error ($RMSE$) can be calculated from:

$$RMSE = \sqrt{\frac{\sum_{i=1}^{M}\left(x^{i}_{Theoretical} - x^{i}_{Experimental}\right)^{2}}{M}} \qquad (42)$$

where $x^{i}_{Theoretical}$ (respectively $x^{i}_{Experimental}$) is the expected theoretical (respectively experimental) value and M is the number of experimental values. Tables 1 and 2 consolidates the $RMSE$ values for the selected frequencies in the case of the single cavity and the periodic array respectively. The $RMSE$ values are less than 0.16 in both cases, thereby confirming close concordance between the analytical model and the experiment.

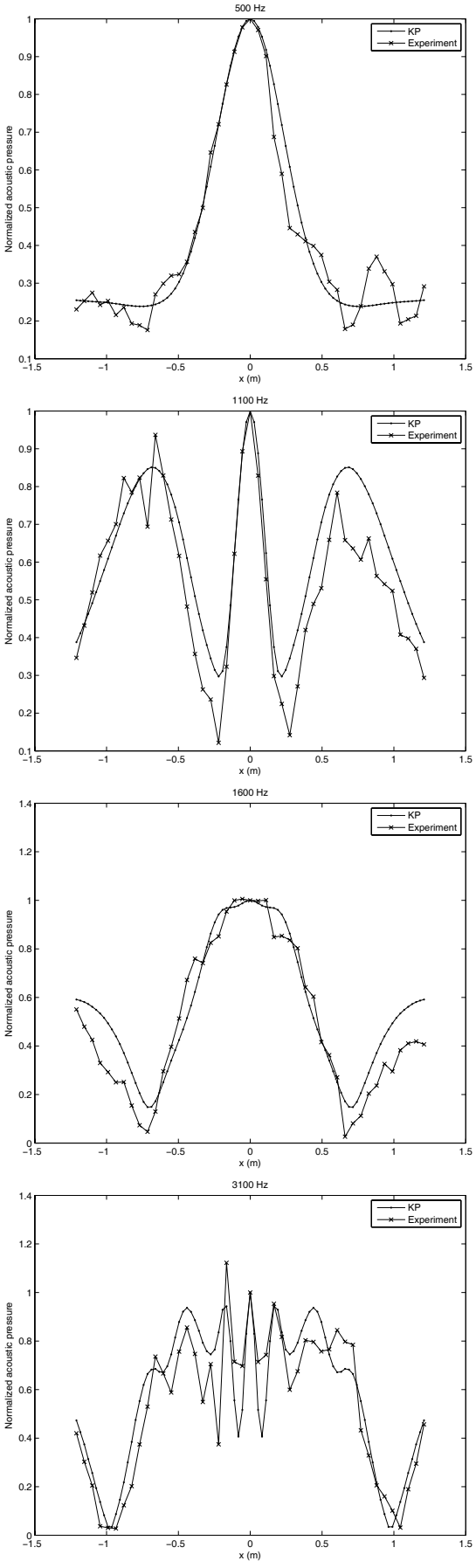

Figure 4: Normalized acoustic pressure at $0.2\,m$ above the studied single cavity for different frequencies

4 Conclusion

An investigation of the acoustic wave scattering by an aperiodic array formed by N parallel rectangular cavities with

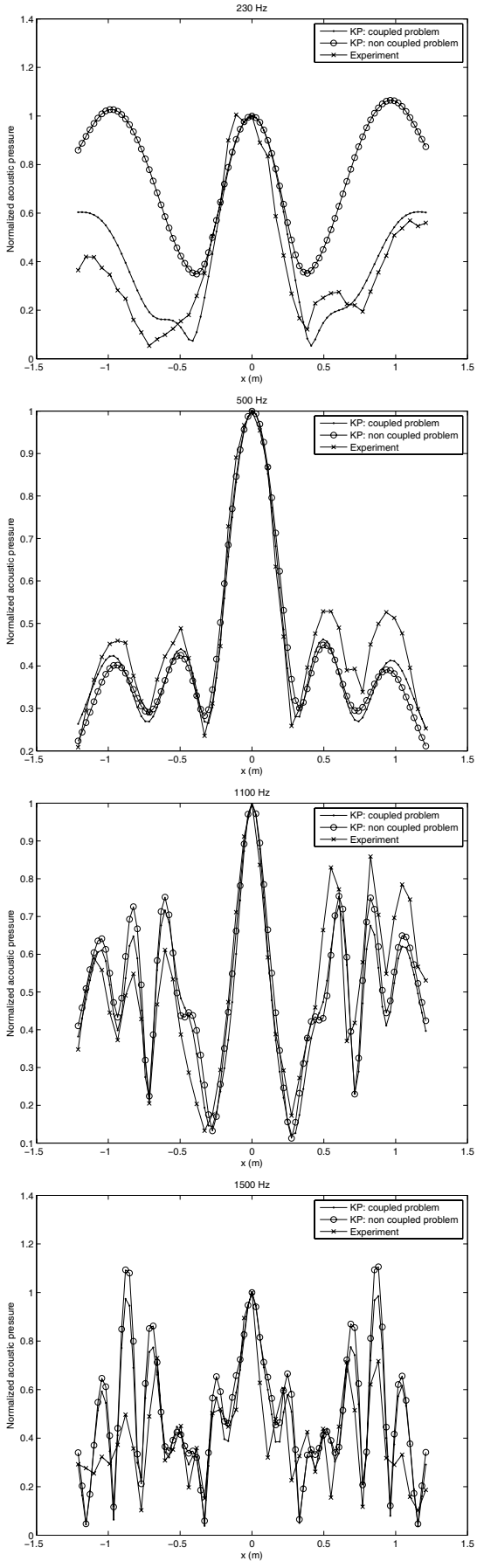

Figure 5: Normalized acoustic pressure at 0.2 m above the periodic array for different frequencies

Frequency	500 Hz	1100 Hz	1600 Hz	3100 Hz
$RMSE$	0.05	0.11	0.10	0.13

Table 1: Relative root mean square errors of the study model for the single cavity.

Frequency	230 Hz	500 Hz	1100 Hz	1500 Hz
$RMSE$	0.11	0.06	0.10	0.16

Table 2: Relative root mean square errors of our model for the periodic array.

different sizes and spacings was performed using KP method. A conparaison between the analytical model and experiment was performed for one cavity and for a periodic array of three cavities. Good concordance was obtained for various frequencies. The $RMSE$ is still low at the highest frequency, so we are hopeful that the model will remain valid above 1500 Hz, approaching the highest possible computing capacity.

It was seen that the coupling between the cavities decrease with frequency. In our experiments, coupling terms were highlighted at 230 Hz. From 500 Hz, and even for close cavities as shown in our study, the coupling becomes relatively negligible.

The study model separates the various existing fields above an aperiodic array of rectangular cavities, namely the incident, the specular reflected and the diffracted fields. This makes it possible to calculate the scattering coefficient of different arrays formed by parallel rectangular cavities. This could lead to finding an optimal configuration giving a high scattering coefficient.

References

[1] K.Hongo, H.Serizawa, "Diffraction of an acoustic plane wave by a rectangular hole in an infinitely large rigid screen", *The Journal of the Acoustical Society of America* **106**, 29-35 (1999)

[2] H.Serizawa, K.Hongo, "Evaluation of an acoustic plane wave transmitted through a rectangular hole in a thick hard screen", *Wave Motion* **36**, 103-117 (2002)

[3] M.Hill, I.Robinson, "d2lri: A nonadaptive algorithm for two-dimensional cubature", *Journal of Computational and Applied Mathematics* **112**, 121-145 (1999)

[4] J.S. Suh, P.A. Nelson, "Measurement of transient response of rooms and comparison with geometrical acoustic models", *The Journal of the Acoustical Society of America* **105**, 2304-2317 (1999)

[5] K. Hongo, N. Furusawa, H. Horis, "Two-dimensional multiple scattering for n slit array", *Electronics and Communications in Japan (Part I: Communications)* **63** 89-96 (1980)

[6] K. Hongo, "Radiation characteristics of flanged parallel-plate waveguide arrays", *Trans. Inst. Electronics and Comm. Engrg in Japan* **61** 161-165 (1978)